



Article

Enhancing Uptake Capability of Green Carbon Black Recycled from Scrap Tires for Water Purification

Jiho Choi ¹ , Jihyun Kang ¹, Huiseong Yang ¹, Sangin Yoon ¹, Jun-Hyun Kim ^{1,2,*}  and Hyun-Ho Park ^{1,*}

¹ Department of Chemistry, Keimyung University, Daegu 42601, Republic of Korea; wlh5090@naver.com (J.C.); kgh8465@gmail.com (J.K.); yhsung7771@naver.com (H.Y.); ydain10@gmail.com (S.Y.)

² Department of Chemistry, Illinois State University, Normal, IL 61790-4160, USA

* Correspondence: jkim5@ilstu.edu (J.-H.K.); rubchem@kmu.ac.kr (H.-H.P.)

Abstract: This study reports on the highly simple fabrication of green carbon black (GCB) generated from scrap tires with acetic acid to improve the adsorption efficiency for water purification, which is thoroughly compared with conventional carbon black (CB) obtained from petrochemicals. Unlike traditional modification processes with strong acids or bases, the introduction of a relatively mild acid readily allowed for the effective modification of GCB to increase the uptake capability of metal ions and toxic organic dyes to serve as effective adsorbents. The morphological features and thermal decomposition patterns were examined by electron microscopy and thermogravimetric analysis (TGA). The surface functional groups were characterized by Fourier transform infrared spectroscopy (FTIR) and X-ray photoelectron spectroscopy (XPS). The structural information (ratio of D-defects/G band-graphitic domains) obtained by Raman spectroscopy clearly suggested the successful fabrication of GCB (I_D/I_G ratio of 0.74), which was distinctively different from typical CB (I_D/I_G ratio of 0.91). In the modified GCB, the specific surface area (S_{BET}) gradually increased with the reduction of pore size as a function of acetic acid content (52.97 m²/g for CB, 86.64 m²/g for GCB, 102.10–119.50 m²/g for acid-treated GCB). The uptake capability of the modified GCB (312.5 mg/g) for metal ions and organic dyes was greater than that of the unmodified GCB (161.3 mg/g) and typical CB (181.8 mg/g), presumably due to the presence of adsorbed acid. Upon testing them as adsorbents in an aqueous solution, all these carbon materials followed the Langmuir isotherm over the Freundlich model. In addition, the removal rates of cationic species (>70% removal of Cu²⁺ and crystal violet in 30 min) were much faster and far greater than those of anionic metanil yellow (<40% removal in 3 h), given the strong electrostatic interactions. Thus, this work demonstrates the possibility of recycling waste tires in the powder form of GCB as a cost-effective and green adsorbent that can potentially substitute traditional CB, and the modification strategy provides a proof of concept for developing simple fabrication guidelines of other carbonaceous materials.

Keywords: green carbon black; scrap tire; adsorbent; cation and anion dye; metal ion



Citation: Choi, J.; Kang, J.; Yang, H.; Yoon, S.; Kim, J.-H.; Park, H.-H. Enhancing Uptake Capability of Green Carbon Black Recycled from Scrap Tires for Water Purification. *Coatings* **2024**, *14*, 389. <https://doi.org/10.3390/coatings14040389>

Academic Editor: Deling Yuan

Received: 29 February 2024

Revised: 24 March 2024

Accepted: 25 March 2024

Published: 27 March 2024



Copyright: © 2024 by the authors. Licensee MDPI, Basel, Switzerland. This article is an open access article distributed under the terms and conditions of the Creative Commons Attribution (CC BY) license (<https://creativecommons.org/licenses/by/4.0/>).

1. Introduction

Carbon black (CB) is pure elemental carbon in a powder form that is typically produced by the incomplete combustion of heavy petrochemicals under controlled conditions [1–5]. Given its unique physicochemical properties, CB has served as an essential filler for tires, plastics, protective materials, electronic devices, and purification systems. In contrast to conventional CB, green carbon black (GCB) has been extracted from scrap tires via sequential anaerobic pyrolysis and a controlled pulverization process, but has shown somewhat inferior overall physical properties for practical applications [6–10]. To overcome one of the properties associated with limited surface areas, developing a simple strategy to regulate the structural features of the GCB helps to improve the uptake capability to serve as a potential adsorbent. Thus, investigating the effective modification and examining

its removal efficiency for organic and inorganic species can allow for the continuous recyclability of GCB as a sustainable product (i.e., eco-friendly CB) in water purification.

In this study, GCB obtained from waste passenger car tires is fabricated to possess an uptake capability as good as or better than conventional CB to serve as an effective adsorbent for metal ions and toxic organic dyes in water. Along with CB, the most popular carbon-based adsorbent or filter material is activated carbon (AC) generated from natural mineral products (e.g., coconut, coal, and animal bones) because of its high surface area and removal efficiency of various contaminants [11–14]. Due to the relatively high cost of AC, much less expensive adsorbents are being investigated for the surface modification of carbonaceous materials [6,15,16]. As scrap tires are a serious waste product that are generated on a global scale, demonstrating the possibility of employing GCB as an adsorbent can provide a method for recycling an almost unlimited resource that can replace the conventional CB and AC in water purification. Thus, the proper modification of GCB can offer several attractive aspects over CB, allowing for the development of economical (i.e., cheaper), green (i.e., significantly reducing CO₂ emission during production), and sustainable sources of adsorbent materials.

Instead of utilizing conventional fabrication approaches for carbonaceous materials with strong acids or bases [8,17–19], GCB is treated with varying concentrations of a mild acid to alter its physicochemical properties and was tested as an adsorbent to remove various contaminants in water [14,20]. After the acid treatment, the structural features and compositional properties were thoroughly compared with CB and GCB. Subsequently, the adsorption capability of the acid-modified GCB was also evaluated with several adsorbates (e.g., metal ions, and cationic/anionic organic dyes). In addition, comparing the adsorption isotherm with CB and GCB allows for understanding their intrinsic roles as adsorbents. As such, this study offers a simple strategy for upcycling troublesome waste tires in the form of adsorbing materials that are cost-efficient, green, and sustainable in water purification.

2. Materials and Methods

2.1. Materials

The traditional carbon black (CB) and green carbon black (GCB) used in the study were the non-polluting and high modulus types of semi-reinforcing furnace black, respectively (N774, OCI Co. and 774G-equivalent to conventional CB, LD Carbon Co., Seoul, Republic of Korea). Acetic acid and CuSO₄·5H₂O, crystal violet (CV), and metanil yellow (MY) were used as purchased.

2.2. Modification of GCB

The modification of GCB was carried out in batch experiments using the following conditions: 20 g of GCB was suspended and mixed in 500 mL of acetic acid solutions (e.g., 0.1 M, 0.2 M, and 0.5 M). Upon complete incubation overnight, GCB was then fully precipitated. After decanting the top solution, the precipitate was vacuum filtered and washed with pure water. The resulting black powder was placed in an oven at 100 °C overnight to serve as an adsorbent.

2.3. Adsorption Test for CB, GCB, and Acid Treated GCB

The CB-based materials were used as adsorbents in the removal of metal ions (i.e., Cu²⁺) and toxic dyes (i.e., CV, a recalcitrant dye existing in the environment, and MY, a yellow azo dye possessing toxicity to the liver, brain, and reproductive organs) [21,22] via batch adsorption experiments. A standard solution was prepared by dissolving each compound in water. A serial dilution was performed to prepare additional standard solutions for calibration curves. For the adsorption test, a series of CB materials (0.1 g–1.0 g) was suspended and mixed in 40 mL of dye solution (e.g., 80 ppm for CV) to initially determine the proper amount of the adsorbents as a function of time. For the precise determination and comparison of the removal (%) in a short period of time, the process was completed using a 10-fold lower concentration of dyes (or Cu²⁺ ions). An

aliquot of solution was taken at fixed time intervals and filtered through a cellulose acetate membrane prior to analysis. The resulting absorbance (measured with UV-Vis or atomic absorption spectrometry) was compared to the corresponding standard curve using the Beer-Lambert law [11,12,23].

2.4. Characterization

Fourier transform infrared spectra (QATR-S FTIR Spectrometer, Shimadzu, Kyoto, Japan) of CB-based materials were obtained in the scan range of 600–4000 cm^{-1} using an attenuated total reflection (ATR) sampling device. Raman spectrometry (ProRaman-L-785B, Enwave Optronics, Irvine, CA, USA) was used to acquire additional vibrational spectra. The 785 nm laser excitation source at ~10 mW was focused on the CB powder mounted on gold nanoparticle-loaded plasmonic filter paper. Spectra were obtained with a 30 s integration time, and the auto-baseline function was turned on during the measurements. The thermal degradation pattern of the CB powder was also examined with a dual thermogravimetric analyzer and differential scanning calorimetry (TGA-DSC, SDT Q600, TA Instruments, New Castle, DE, USA). A small quantity (3–5 mg) of the powder was loaded onto an alumina pan for the measurements using the following conditions (pre-heated at 80 °C for 10 min, ramping temperature of 20 °C/min under 50 mL/min N_2 gas). The distribution and morphology of the CB powder was examined using a field emission scanning electron microscope (FESEM, Zeiss Sigma 300 VP, Carl Zeiss, White Plains, NY, USA) equipped with a Gemini column, capable of operating at low voltages (i.e., 1–2 kV). The powder samples were firmly mounted onto carbon tape prior to the measurement. X-ray photoelectron spectrometers (XPS, Nexsa G2, Thermo Scientific, Waltham, MA, USA) equipped with a monochromatic Al X-ray source (1486.6 eV) was used to examine the chemical compositions of the CB powder samples. As the powder samples were loaded onto a clean tape, all spectra were calibrated using the C 1s peak at 285 eV. The surface charge of CB-based powder was examined by a zeta potential analyzer (Zetasizer Nano, Malvern Panalytical Ltd., Malvern, UK). The sample solution (~20 mg in 30 mL water) was placed in disposable folded capillary cells and equilibrated for 2 min at 25 °C prior to analysis. The data were collected using an average of five measurements. The specific surface area of the CB powder was determined by Brunauer-Emmett-Teller (BET) analysis using the N_2 -based adsorption and desorption isotherms (Quadrasorb-SI, Quantachrome Instruments, Boynton Beach, FL, USA). An atomic absorption spectrophotometer (AAAnalyst 200, Perkin Elmer, Waltham, MA, USA) equipped with a copper hollow cathode lamp (324.8 nm) was used to determine Cu^{2+} ions before and after the treatment with CB-based adsorbents. Based on the calibration curve using standard solutions of $\text{CuSO}_4 \cdot 5\text{H}_2\text{O}$ in water (1 ppm–100 ppm), the amount of Cu^{2+} ions was determined as a function of time. An UV-Visible spectrophotometer (Agilent 843, Agilent Technologies, Santa Clara, CA, USA) was used to collect absorption spectra of dyes and metal ions (300 nm–1100 nm). The three analytes we selected possess distinctively different absorption maxima to avoid any spectral overlaps. Based on the absorption patterns, adsorption isotherms were calculated to quantify the affinity degree of the adsorbate for the adsorbent using the following two representative models (i.e., Langmuir and Freundlich) [24–26].

The Langmuir isotherm is presented as following.

$$\frac{1}{q_e} = \frac{1}{K_L q_{\max}} \times \frac{1}{C_e} + \frac{1}{q_{\max}} \quad (1)$$

where q_e : adsorption capacity (mg/g), K_L : Langmuir constant, q_{\max} : maximum adsorption capacity (mg/g), and C_e : equilibrium concentration (mg/L). The q_{\max} and K_L constant values were determined from the linear regression line of Langmuir isotherm graph. In addition, the separation factor (R_L) was calculated using the following equation:

$$R_L = \frac{1}{1 + C_i + K_L} \quad (2)$$

where, R_L : dimensionless Langmuir constant and C_i : initial concentration.
The Freundlich isotherm is presented as following.

$$\text{Log } q_e = \text{Log } K_f + \frac{1}{n} \text{Log } C_e \quad (3)$$

where q_e adsorption capacity (mg/g), K_f : Freundlich's constant, and $1/n$: adsorption intensity, and C_e : the equilibrium concentrations of adsorbate (mg/L).

These models can describe the relationships between the amount of adsorbate on an adsorbent and the concentration of adsorbate in solution at equilibrium conditions.

3. Results

3.1. Structural and Compositional Properties of CB, GCB, and Acid-Treated GCB

Prior to characterizing acetic acid-treated GCB, the structural characteristics of CB and GCB were examined in digital photos and FE-SEM images (Figure 1). The incomplete combustion of heavy petroleum products in a conventional furnace black process resulted in relatively uniform and sub-millimeter particulate CB with a smooth surface that can be easily popped open. The GCB sample obtained from the waste tires via thermal pyrolysis exhibited a somewhat coarse and detectably less-uniform powder. The SEM images generally showed that the CB powder appeared to be more porous than the GCB. The surface of GCB was slightly rougher and had a smaller particulate form than that of the CB powder. Upon treatment with acetic acid, the GCB powder seemed to have a somewhat finer appearance, but the coagulated particles displayed a slightly smaller pore size. Overall, these CB-based materials generally exhibited some cavities, cracks, and pores that could potentially possess high surface areas.

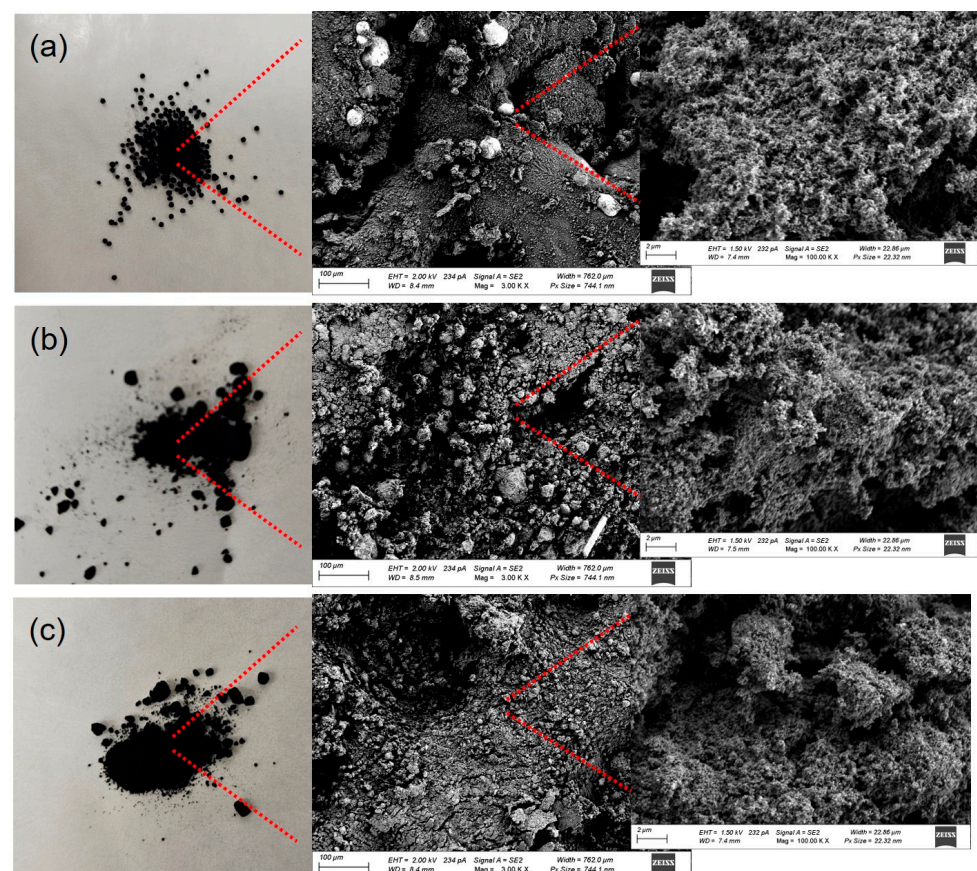


Figure 1. Digital photos and SEM images of (a) CB, (b) GCB, and (c) acid-treated GCB (0.5 M acetic acid).

An FTIR/ATR vibrational spectrophotometer was used to examine the surface functional groups of CB, GCB, and acid-treated GCB (Figure 2a). Interestingly, strong peaks were hardly observed for the conventional CB powder except the adventitious CO_2 peak at $2200\text{--}2300\text{ cm}^{-1}$, which is very close to that described in previous literature [7,27,28]. Although the GCB powder exhibited similar vibration patterns [7,29], the acid-treated GCB displayed a few additional peaks: at 2950 cm^{-1} (CH_3 stretching), 1623 cm^{-1} ($\text{C}=\text{C}$ asymmetrical stretching), 1520 cm^{-1} for the acyl species (COO -anti-symmetrically stretching), and $1350\text{--}1420\text{ cm}^{-1}$ (CH_3 symmetric deformation and COH bending) [14,30]. The presence of these detectable peaks evidently suggested the presence of relatively strong physical interactions between acetic acid and GCB, where the acid molecules could play an important role in inducing attractive interactions with metal ions and dye molecules. Raman spectra were also collected to evaluate the main graphitic backbone of carbon-based materials (Figure 2b). All three powder samples exhibited very similar patterns of D band (1330 cm^{-1} for disordered/defective aromatic rings) and G band (1590 cm^{-1} for the graphitic $\text{C}=\text{C}$ stretching of sp^2 hybridized carbon) [10,31–33]. Although these bands appeared to be mostly unchanged, the relative intensities (i.e., ratios) of the D and G bands (I_D/I_G) could explain the disordered degree of carbon material (i.e., graphitization of carbons) [32,34]. Generally, the CB powder showed a slightly higher I_D/I_G (0.91) value than that of GCB (0.74), implying a higher amorphous feature. The ratio of the acid-treated GCB appeared to be marginally decreased (0.65), indicating a slight change in the graphitic structure of the GCB.

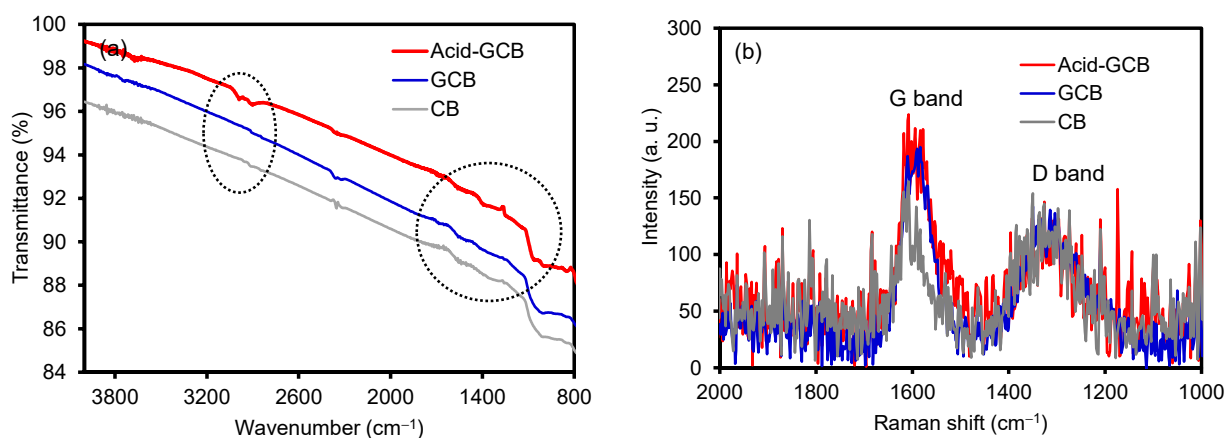


Figure 2. Vibrational spectra of CB, GCB, and acid-treated GCB (0.5 M acetic acid) using: (a) FTIR; (b) Raman, spectrophotometers.

Furthermore, XPS analysis was carried out to confirm the presence of acetic acid on GCB (Figure 3 and Supplementary Figure S1). From the survey scans, the conventional CB only showed two peaks at 284.0 eV ($\text{C } 1s$) and 532 eV ($\text{O } 1s$), but GCB and acid-treated GCB displayed several additional peaks corresponding to $\text{Zn } 2p$, $\text{Mn } 2p$, $\text{S } 2p$, and $\text{Si } 2p$ [35,36]. The presence of these distinctively different peaks confirmed that the recycled CB (i.e., GCB) contains a small amount of other chemical elements from scrap tires. The subsequent treatment of GCB with 0.1 M , 0.2 M , and 0.5 M acetic acid gradually resulted in an increase in oxygen (O) content around the GCB surface. Due to the adsorption of acetic acid onto GCB, the $\text{O } 1s$ peak has two components at $\sim 532\text{ eV}$ and $\sim 533\text{ eV}$ assigned to oxygen in the CB backbone and acetic acid, respectively [37,38]. Likewise, an additional peak appeared at $\sim 288\text{ eV}$ for carboxyl carbons from acetic acid, along with the original carbon peak at $\sim 284\text{ eV}$ (slightly shifted) for the methyl and CB backbones. The introduction of relatively hydrophilic molecules onto GCB can potentially improve the overall dispersion in an aqueous solution, which was supported by the changes of surface charges examined by zeta potential measurements (Figure S2).

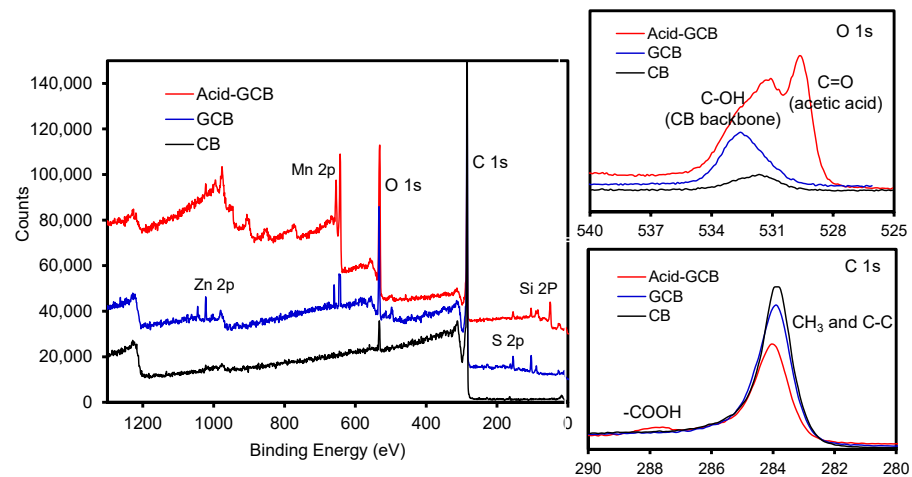


Figure 3. XPS survey and detail scans of CB, GCB, and acid-treated GCB (0.5 M acetic acid).

3.2. Thermal and Adsorption Properties of CB, GCB, and Acid-Treated GCB

Thermogravimetric analysis (TGA) was additionally carried out in an N_2 gas environment to monitor the weight loss patterns of CB, GCB, and acid-treated GCB (Figures 4a and S3). The CB powder showed barely any reduction in weight as the temperature increased up to $800\text{ }^\circ\text{C}$, which was comparable to other conventional CB [2,39–41]. However, the GCB powder initially displayed similar thermal decomposition patterns but discernible weight loss ($\sim 2\text{ wt}\%$) starting around $600\text{ }^\circ\text{C}$, presumably due to the presence of a complex mixture of materials (e.g., Al, Cl, Zn, and Si) during the recovering process from scrap passenger tires [8,42]. The acid-treated GCB powder showed much greater thermal decomposition starting over $420\text{ }^\circ\text{C}$ where the char amount was approximately $9\text{ wt}\%$ higher than the initial GCB. This notable weight loss could be associated with the acid-induced fabrication of CB reported by other groups [8,43,44]. To confirm the modification of GCB with acetic acid, several parameters (e.g., surface area, pore size, pore volume) [13,25] were examined by the Brunauer-Emmett-Teller (BET) measurements using N_2 gas adsorption-desorption isotherms (Figure 4b and Table S1). The specific surface areas (S_{BET}) of the CB, GCB, and acid-treated GCB were examined to be $52.97\text{ m}^2/\text{g}$, $86.64\text{ m}^2/\text{g}$, and $119.50\text{ m}^2/\text{g}$, respectively. On the other hand, the average pore sizes (33.31 nm for CB, 25.91 nm for GCB, and 20.51 nm for 0.5 M acid-treated GCB) were inversely proportional to the S_{BET} values, which supported the observations of the SEM images above. The representative isotherm curves (i.e., type IV with mesoporous features) were slightly different with comparable hysteresis loops, suggesting that the acid treatment moderately influenced the overall surface area and pore structure of GCB.

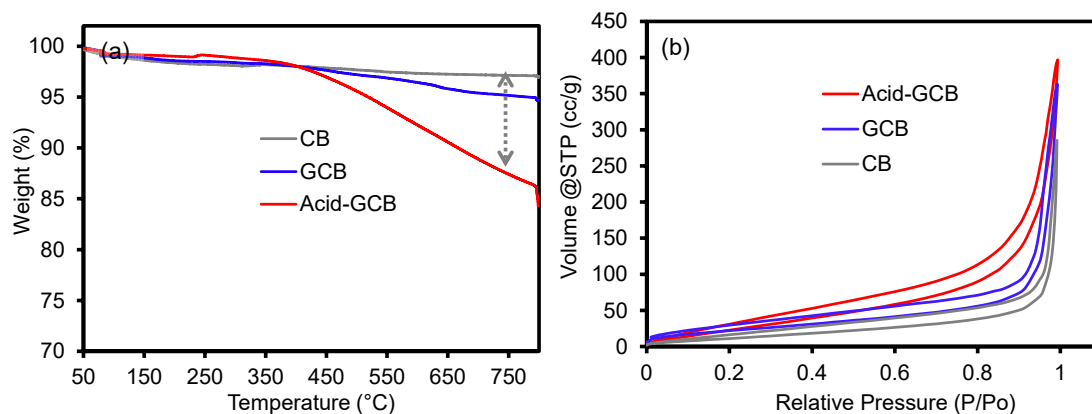


Figure 4. (a) Weight loss patterns, and (b) BET N_2 adsorption isotherms, of: CB, GCB, and acid-treated GCB (0.5 M acetic acid).

3.3. Removal of Organic Dyes and Metal Ions Using CB, GCB, and Acid-Treated GCB (0.5 M Acetic Acid)

After thoroughly examining their physicochemical properties, these CB derivatives were tested for the removal of common metal ions and toxic dyes in an aqueous solution (Figures 5 and S4). The removal (%) of the cation (i.e., crystal violet, CV), the anion (i.e., metanil yellow dyes, MY), and metal ions (i.e., Cu^{2+}) was monitored by examining their molecular and atomic absorption peaks (CV at 591 nm, MY at 449 nm, and $\text{Cu}(\text{II})$ at 324.8 nm), which were compared to the standards (Figures S5 and S6). Given the diverse functional groups of CB-based materials, these adsorbents could effectively remove various adsorbates from water. As expected, the overall removal (%) of CV dye and Cu^{2+} ions (cationic species) were notably faster than MY dye (anionic species). Particularly, the acid-treated GCB (i.e., 0.5 M acetic acid) clearly showed much quicker removal and higher uptake capability, presumably caused by the physically adsorbed acetic acid to induce electrostatic interactions across the surface of the GCB [14]. Specifically, GCB has shown a slightly higher SBET value than that of the conventional CB, but CB displayed a moderately faster removal rate than the GCB, probably due to the somewhat different surface compositions (e.g., slightly fewer C-OH groups) and absence of counter ions (shown in XPS in Figure 3). The degree of removal rate was detectably faster for the acid-treated GCB compared to that of other CB materials. These experimental results evidently suggested the possibility of utilizing the acid-treated GCB obtained from scrap tires that can replace the conventional CB-based filter material in water purification.

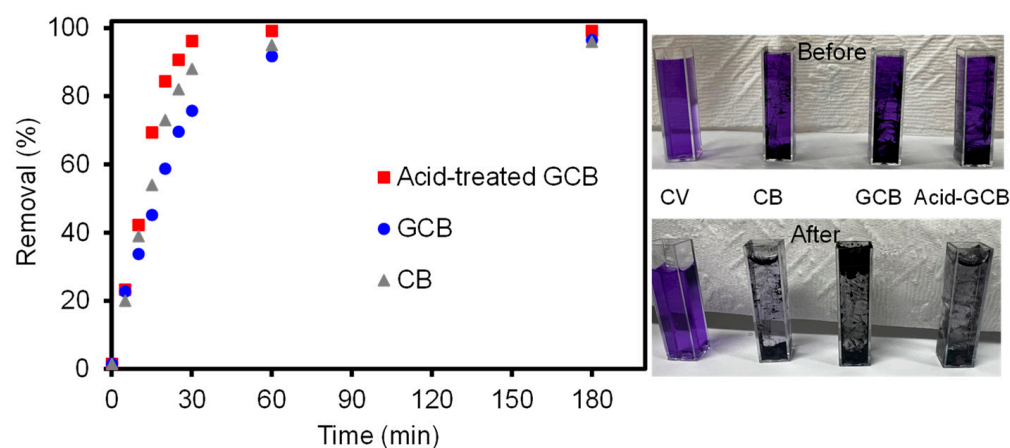


Figure 5. Removal (%) of CV using 0.03 g of CB, GCB, and acid-treated GCB (0.5 M acetic acid) as a function of time CV solution.

Furthermore, the equilibrium adsorption isotherms of the cationic CV dye were examined using CB, GCB, and acid-treated GCB (Figure 6). The adsorption of the adsorbates increases as a function of the adsorbent amount, where the acid-treated GCB ($q_{\text{max}} = 312.5 \text{ mg/g}$) uptakes a much greater amount than CB ($q_{\text{max}} = 181.8 \text{ mg/g}$) and GCB ($q_{\text{max}} = 161.3 \text{ mg/g}$). Among many adsorption parameters, two representative Langmuir and Freundlich isotherms were compared by calculating the slope and intercept of the linear plots of C_e/q_e vs. C_e and $\ln q_e$ vs. $\ln C_e$ (Table S2). The correlation coefficient for these CB-based materials indicated slightly better agreement with the Langmuir isotherm than the Freundlich model. The Langmuir isotherm assumes that these CB-based materials induce monolayer adsorption of the dye on somewhat homogeneous sites, mainly due to the physical adsorption process between the negatively-charged surface functional groups and the positive characteristics of adsorbates.

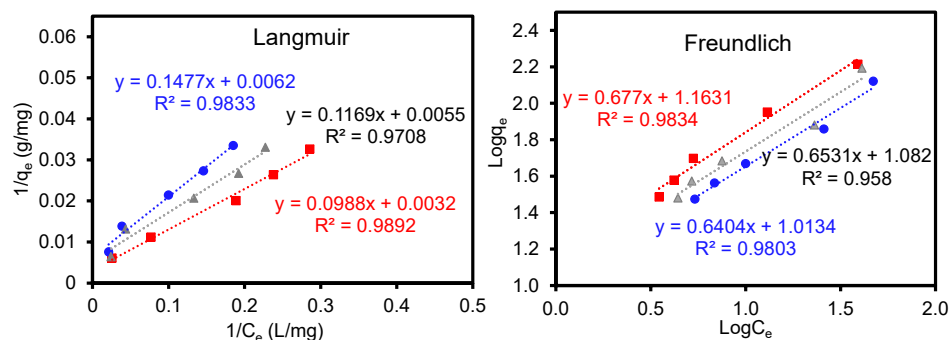


Figure 6. Adsorption isotherms of CV onto CB, GCB, and acid-treated GCB (0.5 M acetic acid).

Similarly, the overall removal (%) of anion MY dye and Cu^{2+} ions were examined using the CB, GCB, and acid-treated GCB (Figure S7). As the molar absorptivity of MY and Cu^{2+} was detectably lower than CV [26,45], the initial concentrations used in the experiment were slightly higher for accurate measurements. However, the UV-Vis analysis of Cu^{2+} ions at high concentrations before and after the treatment using the CB-based adsorbents made it difficult to obtain meaningful information under our experimental conditions. Thus, an atomic absorption spectrometer (AAS) was employed for the accurate determination of Cu^{2+} ions. The removal (%) of the conventional CB was relatively greater than that of the GCB due to the presence of more anionic functional groups without counter metal ions. With the use of the acid-treated GCB, the removal of Cu^{2+} ions were promoted by the stronger interactive forces. All CB-based adsorbents displayed similar removal patterns of Cu^{2+} ions, where the degree of removal (%) for the acid-treated GCB was faster than the CB and GCB. In the case of the anion MY, all CB adsorbents showed notably slower removal rates and possessed relatively poor adsorption capacity given the anionic nature of the MY adsorbate. Particularly, the acid-treated GCB displayed the worst performance, presumably due to the presence of strong electrostatic repulsions (zeta potential changes shown in Figure S2). Although these CB-materials with abundant anionic carboxylate groups induced an unfavorable adsorption process, it appears that attractive driving forces associated with hydrogen and π - π interactions still exist between the adsorbent and adsorbate at instantaneous equilibrium conditions [46,47]. More in-depth studies are underway. Although the GCB obtained from passenger scrap tires has a limited surface area and functionality, the introduction of mild acid successfully induced the preferential adsorption of various contaminants, particularly cationic species. Thus, the surface modification of the GCB-based adsorbent plays an important role in water purification [48]. As the pH of an aqueous solution can easily be regulated ($\text{pH} > \text{pKa}$ of acetic acid) with inorganic bases, negatively charged surfaces can readily promote the strong adsorption of cationic species via attractive electrostatic interactions in addition to typical attractive forces (e.g., van der Waals, hydrogen bonding, and π - π interactions).

4. Conclusions

Unlike conventional CB, GCB obtained from waste tires initially exhibited slightly poor dispersion and limited surface area. Proper treatment of GCB with a mild acid resulted in structural and compositional changes. SEM and BET characterizations confirmed the gradual changes in overall morphology, specific surface areas, and pore size distributions. FTIR, Raman, TGA, and XPS clearly explained the distinctively different compositional information. In addition, the relative dispersity and wettability of the modified GCB appeared to increase in water. Strategic property changes for GCB played an important role in positively influencing the degree of uptake capability for organic dyes and heavy metal ions. However, the equilibrium adsorption isotherms for all CB-based materials followed the Langmuir model regardless of the modification. The ability to effectively regulate GCB to possess adsorption properties as good as or better than conventional CB will allow for the development of a new alternative for water purification. Therefore,

strategically regulating the physical properties of GCB could potentially provide guidelines to upcycle scrap tires as a highly economical, green, and sustainable adsorbent material. The study not only underscores the scientific aspects of CB treatment but also provides eco-conscious endeavors for industrial applications.

Supplementary Materials: The following supporting information can be downloaded at: <https://www.mdpi.com/article/10.3390/coatings14040389/s1>, Figure S1: XPS survey and detail scans of CB, GCB, and acid-treated GCB (0.1 M, 0.2 M, and 0.5 M acetic acid); Figure S2: Digital photo and zeta potential of CB, GCB, and acid-treated GCB (20 mg) in 30 mL water; Figure S3. Derivative TGA curves of CB, GCB, and acid-treated GCB as a function of time; Figure S4. UV-Vis spectra of CV as a function of concentration and the corresponding calibration curve; Figure S5. UV-Vis spectra of MY as a function of concentration and the corresponding calibration curves (digital photos show the dye solutions before and after treatment with CB-based adsorbents overnight); Figure S6. Calibration curve of Cu^{2+} ions obtained by atomic absorption spectroscopy (AAS) and the representative Cu^{2+} solution after the treatment with CB-based adsorbents; Figure S7. Removal (%) of MY (a) and Cu^{2+} (b) using CB, GCB, and acid-treated GCB (0.03 g) as a function of time; Table S1. Specific surface area (S_{BET}), pore volume, and pore size analysis of CB, GCB, and acetic acid-treated GCB via N_2 gas adsorption-desorption isotherms; Table S2. Langmuir and Freundlich isotherm parameters for the removal of CV using CB, GCB, and acid-treated GCB.

Author Contributions: Conceptualization: J.C., S.Y., J.-H.K. and H.-H.P.; Methodology: S.Y. and H.-H.P.; Investigation and formal analysis: J.C., J.K., H.Y. and H.-H.P.; Writing—original draft preparation: J.C. and J.-H.K.; writing—review and final editing: J.-H.K. and H.-H.P.; Supervision and project administration: J.-H.K. and H.-H.P.; Funding acquisition: H.-H.P. All authors have read and agreed to the published version of the manuscript.

Funding: This research was supported by the Bisa Research Grant of Keimyung University in 2023. The FESEM multi-user facility was acquired with the support from the Division of Material Research (DMR), National Science Foundation (NSF) (Award # 2116612).

Institutional Review Board Statement: Not applicable.

Informed Consent Statement: Not applicable.

Data Availability Statement: Data is available upon request.

Acknowledgments: We gratefully acknowledge the support from the Bisa Research Grant of Keimyung University in 2023 and the Department of Chemistry of Illinois State University. We also thank LD Carbon Co., Ltd. for its generous donation of green carbon black.

Conflicts of Interest: The authors declare no conflicts of interest.

References

1. Burgaz, E.; Gencoglu, O.; Göksüzoğlu, M. Carbon black reinforced natural rubber/butadiene rubber and natural rubber/butadiene rubber/styrene-butadiene rubber composites: Part II. Dynamic mechanical properties and fatigue behavior. *Res. Eng. Struct. Mater.* **2019**, *5*, 233–247. [[CrossRef](#)]
2. Khudoynazarov, F.; Nurmanov, S.; Yakubo, Y. The composition and thermodynamic properties of pyrolytic carbon black. *Int. J. Mater. Chem.* **2022**, *12*, 32–38.
3. Saini, D.; Gunture; Kaushik, J.; Aggarwal, R.; Tripathi, K.M.; Sonkar, S.K. Carbon nanomaterials derived from black carbon soot: A review of materials and applications. *ACS Appl. Nano Mater.* **2021**, *4*, 12825–12844. [[CrossRef](#)]
4. Toth, P.; Vikström, T.; Molinder, R.; Wiinikka, H. Structure of carbon black continuously produced from biomass pyrolysis oil. *Green Chem.* **2018**, *20*, 3981–3992. [[CrossRef](#)]
5. Wang, J.; Man, H.; Sun, L.; Zang, S. Carbon black: A good adsorbent for triclosan removal from water. *Water* **2022**, *14*, 576. [[CrossRef](#)]
6. Costa, S.M.R.; Fowler, D.; Carreira, G.A.; Portugal, I.; Silva, C.M. Production and upgrading of recovered carbon black from the pyrolysis of end-of-life tires. *Materials* **2022**, *15*, 2030. [[CrossRef](#)] [[PubMed](#)]
7. Dwivedi, C.; Manjare, S.; Rajan, S.K. Recycling of waste tire by pyrolysis to recover carbon black: Alternative & environment-friendly reinforcing filler for natural rubber compounds. *Compos. Part B* **2020**, *200*, 108346.
8. González-González, R.B.; González, L.T.; Iglesias-González, S.; González-González, E.; Martínez-Chapa, S.O.; Madou, M.; Alvarez, M.M.; Mendoza, A. Characterization of chemically activated pyrolytic carbon black derived from waste tires as a candidate for nanomaterial precursor. *Nanomaterials* **2020**, *10*, 2213. [[CrossRef](#)] [[PubMed](#)]

9. Lee, S.-H.; Kim, J.-H.; Park, H.-H. Upcycling green carbon black as a reinforcing agent for styrene–butadiene rubber materials. *RSC Adv.* **2022**, *12*, 30480–30486. [[CrossRef](#)]
10. Yang, F.; Liang, S.; Wu, H.; Yue, C.; Yan, H.; Wu, H.; Chen, X.; Zhang, J.; Yan, S.; Duan, Y. Upgrading the pyrolysis carbon black from waste tire by hybridization with cellulose. *Ind. Eng. Chem. Res.* **2022**, *61*, 6512–6520. [[CrossRef](#)]
11. Alkhabbas, M.; Al-Ma'abreh, A.M.; Edris, G.; Saleh, T.; Alhmoode, H. Adsorption of anionic and cationic dyes on activated carbon prepared from oak cupules: Kinetics and thermodynamics studies. *Int. J. Environ. Res. Public Health* **2023**, *20*, 3280. [[CrossRef](#)] [[PubMed](#)]
12. Suhas; Kushwaha, S.; Tyagi, I.; Ahmed, J.; Chaudhary, S.; Chaudhary, M.; Inbaraj, B.S.; Goscianska, J.; Karri, R.R.; Sridhar, K. Adsorptive analysis of azo dyes on activated carbon prepared from *Phyllanthus emblica* fruit stone sequentially via hydrothermal treatment. *Agronomy* **2022**, *12*, 2134. [[CrossRef](#)]
13. Valdivia, A.E.O.; Osorio, C.M.; Rodríguez, Y.M.V. Preparation of activated carbon from coffee waste as an adsorbent for the removal of chromium (III) from water. Optimization for an experimental Box-Behnken design. *Chemistry* **2020**, *2*, 2–10. [[CrossRef](#)]
14. Wu, H.; Sun, W.; Wei, H.; Zhao, Y.; Jin, C.; Yang, X.; Rong, X.; Sun, C. Efficient removal of acetic acid by a regenerable resin-based spherical activated carbon. *Water Sci. Technol.* **2021**, *84*, 679–711. [[CrossRef](#)] [[PubMed](#)]
15. El-Maadawy, M.M.; Elzoghby, A.A.; Masoud, A.M.; El-Deeb, Z.M.; El Naggar, A.M.A.; Taha, M.H. Conversion of carbon black recovered from waste tires into activated carbon via chemical/microwave methods for efficient removal of heavy metal ions from wastewater. *RSC Adv.* **2024**, *14*, 6324–6338. [[CrossRef](#)] [[PubMed](#)]
16. Ko, D.C.K.; Mui, E.L.K.; Lau, K.S.T.; McKay, G. Production of activated carbons from waste tire—Process design and economical analysis. *Waste Manag.* **2004**, *24*, 875–888. [[CrossRef](#)] [[PubMed](#)]
17. Acocella, M.R.; Maggio, M.; Ambrosio, C.; Aprea, N.; Guerra, G. Oxidized carbon black as an activator of transesterification reactions under solvent-free conditions. *ACS Omega* **2017**, *2*, 7862–7867. [[CrossRef](#)]
18. Dong, P.; Maneerung, T.; Ng, W.C.; Zhen, X.; Dai, Y.; Tong, Y.W.; Ting, Y.-P.; Koh, S.N.; Wang, C.-H.; Neoh, K.G. Chemically treated carbon black waste and its potential applications. *J. Hazard. Mater.* **2017**, *321*, 62–72. [[CrossRef](#)] [[PubMed](#)]
19. Rehman, A.; Park, M.; Park, S.-J. Current progress on the surface chemical modification of carbonaceous materials. *Coatings* **2019**, *9*, 103. [[CrossRef](#)]
20. Bakr, A.M.; McBain, J.W. The sorption of toluene and acetic acid and their mixtures by carbon. *J. Am. Chem. Soc.* **1924**, *46*, 2718–2725. [[CrossRef](#)]
21. Ghosh, D.; Singha, P.S.; Firdaus, S.B.; Ghosh, S. Metanil yellow: The toxic food colorant. *Asian Pac. J. Health Sci.* **2017**, *4*, 65–66. [[CrossRef](#)]
22. Mani, S.; Bharagava, R.N. Exposure to crystal violet, its toxic, genotoxic and carcinogenic effects on environment and its degradation and detoxification for environmental safety. In *Reviews of Environmental Contamination and Toxicology*; de Voogt, W.P., Ed.; Springer: Cham, Switzerland, 2016; Volume 237, pp. 71–104.
23. Yuan, D.; Yang, K.; Zhu, E.; Li, X.; Sun, M.; Xiao, L.; Hari, Q.; Tang, S. Peracetic acid activated with electro-Fe²⁺ process for dye removal in water. *Coatings* **2022**, *12*, 466. [[CrossRef](#)]
24. Matthews, T.; Majoni, S.; Nyoni, B.; Naidoo, B.; Chiririwa, H. Adsorption of lead and copper by a carbon black and sodium bentonite composite material: Study on adsorption isotherms and kinetics. *Iran. J. Chem. Chem. Eng.* **2019**, *38*, 101–109.
25. Williams, J.H.; Gbadomosi, M.; Greytak, A.B.; Myrick, M.L. Measuring the surface area of carbon black using BET isotherms: An experiment in physical chemistry. *J. Chem. Educ.* **2023**, *100*, 4838–4844. [[CrossRef](#)]
26. Zhai, Q.-Z. Studies of adsorption of crystal violet from aqueous solution by nano mesocellular foam silica: Process equilibrium, kinetic, isotherm, and thermodynamic studies. *Water Sci. Technol.* **2020**, *81*, 2092–2108. [[CrossRef](#)]
27. da Silva, E.L.; Vega, M.R.O.; dos Santos Correa, P.; Cuna, A.; Tancredi, N.; de Fraga Malfatti, C. Influence of activated carbon porous texture on catalyst activity for ethanol electro-oxidation. *Int. J. Hydrogen Energy* **2014**, *39*, 14760–14767. [[CrossRef](#)]
28. Guo, Y.; Zheng, Y.; Huang, M. Enhanced activity of PtSn/C anodic electrocatalyst prepared by formic acid reduction for direct ethanol fuel cells. *Electrochim. Acta* **2008**, *53*, 3102–3108. [[CrossRef](#)]
29. Sugatri, R.I.; Wirasadewa, Y.C.; Saputro, K.E.; Muslih, E.Y.; Ikono, R.; Nasir, M. Recycled carbon black from waste of tire industry: Thermal study. *Microsyst. Technol.* **2018**, *24*, 749–755. [[CrossRef](#)]
30. Colomer, M.T. Straightforward synthesis of Ti-doped YSZ gels by chemical modification of the precursors alkoxides. *J. Sol-Gel. Sci. Technol.* **2013**, *67*, 135–144. [[CrossRef](#)]
31. Gillibert, R.; Magazzù, A.; Callegari, A.; Bronte-Ciriza, D.; Foti, A.; Donato, M.G.; Maragò, O.M.; Volpe, G.; de La Chapelle, M.L.; Lagarde, F.; et al. Raman tweezers for tire and road wear micro- and nanoparticles analysis. *Environ. Sci. Nano* **2022**, *9*, 145–161. [[CrossRef](#)]
32. Jankovská, Z.; Vecer, M.; Koutník, I.; Matejová, L. A case study of waste scrap tyre-derived carbon black tested for nitrogen, carbon dioxide, and cyclohexane adsorption. *Molecules* **2020**, *25*, 4445. [[CrossRef](#)]
33. Kamran, U.; Park, S.-J. Acetic acid-mediated cellulose-based carbons: Influence of activation conditions on textural features and carbon dioxide uptakes. *J. Colloid Interface Sci.* **2021**, *594*, 745–758. [[CrossRef](#)] [[PubMed](#)]
34. Saravanan, M.; Ganesan, M.; Ambalavanan, S. An in situ generated carbon as integrated conductive additive for hierarchical negative plate of lead-acid battery. *J. Power Sources* **2014**, *251*, 20–29. [[CrossRef](#)]
35. Kirakosyan, A.; Lee, D.; Choi, Y.; Jung, N.; Choi, J. Poly(styrene sulfonic acid)-grafted carbon black synthesized by surface-initiated atom transfer radical polymerization. *Molecules* **2023**, *28*, 4168. [[CrossRef](#)] [[PubMed](#)]

36. Pantea, D.; Darmstadt, H.; Kaliaguine, S.; Roy, C. Electrical conductivity of conductive carbon blacks: Influence of surface chemistry and topology. *Appl. Surf. Sci.* **2003**, *217*, 181–193. [[CrossRef](#)]
37. Blanco, Y.S.; Topel, O.; Bajnoczi, E.G.; Werner, J.; Bjorneholm, O.; Persson, I. Chemical equilibria of aqueous ammonium–carboxylate systems in aqueous bulk, close to and at the water–air interface. *Phys. Chem. Chem. Phys.* **2019**, *21*, 12434–12445. [[CrossRef](#)]
38. Nguyen, H.K.K.; Addou, R.; Chukwu, K.C.; Herman, G.S.; Árnadóttir, L. Ambient-pressure X-ray photoelectron spectroscopy study of acetic acid thermal decomposition on Pd (111). *J. Phys. Chem. C* **2023**, *127*, 11472–11480. [[CrossRef](#)]
39. Ahn, D.; Choi, H.-J.; Kim, H.-D.; Yeo, S.Y. Properties of conductive polyacrylonitrile fibers prepared by using benzoxazine modified carbon black. *Polymers* **2020**, *12*, 179. [[CrossRef](#)]
40. Kim, M.I.; Cho, J.H.; Bai, B.C.; Im, J.S. The control of volume expansion and porosity in carbon block by carbon black (CB) addition for increasing thermal conductivity. *Appl. Sci.* **2020**, *10*, 6068. [[CrossRef](#)]
41. Thonglueng, N.; Sirisangsawang, R.; Sukpancharoen, S.; Phetyim, N. Optimization of iodine number of carbon black obtained from waste tire pyrolysis plant via response surface methodology. *Heliyon* **2022**, *8*, e11971. [[CrossRef](#)]
42. Gomez-Hernandez, R.; Panecatl-Bernal, Y.; Mendez-Rojas, M.A. High yield and simple one-step production of carbon black nanoparticles from waste tires. *Heliyon* **2019**, *5*, e02139. [[CrossRef](#)]
43. Bernal, R.A.O.; Olekhnovich, R.O.; Uspenskaya, M.V. Influence of thermal treatment and acetic acid concentration on the electroactive properties of chitosan/PVA-based micro- and nanofibers. *Polymers* **2023**, *15*, 3719. [[CrossRef](#)]
44. Rađenović, A.; Malina, J. Adsorption ability of carbon black for nickel ions uptake from aqueous solution. *Hem. Ind.* **2013**, *67*, 51–58. [[CrossRef](#)]
45. Nath, P.P.; Sarkar, K.; Tarafder, P.; Paul, G. Development of a visible spectrophotometric method for the quantitative determination of metanil yellow in different food samples. *Int. J. Pharma Bio. Sci.* **2013**, *4*, 685–692.
46. Boehm, H.P. Some aspects of the surface chemistry of carbon blacks and other carbons. *Carbon* **1994**, *32*, 759–769. [[CrossRef](#)]
47. Jia, R.-L.; Wang, C.-Y. Adsorption of PtCl_6^{2-} anions on the surface of carbon black. *React. Kinet. Catal. Lett.* **2006**, *88*, 51–56. [[CrossRef](#)]
48. Legocka, I.; Kusmierek, K.; Swiatkowski, A.; Wierzbicka, E. Adsorption of 2,4-D and MCPA herbicides on carbon black modified with hydrogen peroxide and aminopropyltriethoxysilane. *Materials* **2022**, *15*, 8433. [[CrossRef](#)]

Disclaimer/Publisher’s Note: The statements, opinions and data contained in all publications are solely those of the individual author(s) and contributor(s) and not of MDPI and/or the editor(s). MDPI and/or the editor(s) disclaim responsibility for any injury to people or property resulting from any ideas, methods, instructions or products referred to in the content.